Kobe University Repository : Kernel

PDF issue: 2025-12-05

Identification of a Post-translational Modification with Ribitol-Phosphate and Its Defect in Muscular Dystrophy

Kanagawa, Motoi ; Kobayashi, Kazuhiro ; Tajiri, Michiko ; Manya, Hiroshi ; Kuga, Atsushi ; Yamaguchi, Yoshiki ; Akasaka-Manya, Keiko ;…

(Citation)
Cell Reports,14(9):2209-2223

(Issue Date)
2016-03-08

(Resource Type)
journal article

(Version)
Version of Record

(Rights)
©2016 The Authors.
This is an open access article under the CC BY-NC-ND license
(http://creativecommons.org/licenses/by-nc-nd/4.0/)

(URL)
https://hdl.handle.net/20.500.14094/90003339

KOBE UNIVERSITY

Article

Cell Reports

Identification of a Post-translational Modification with Ribitol-Phosphate and Its Defect in Muscular Dystrophy

Graphical Abstract

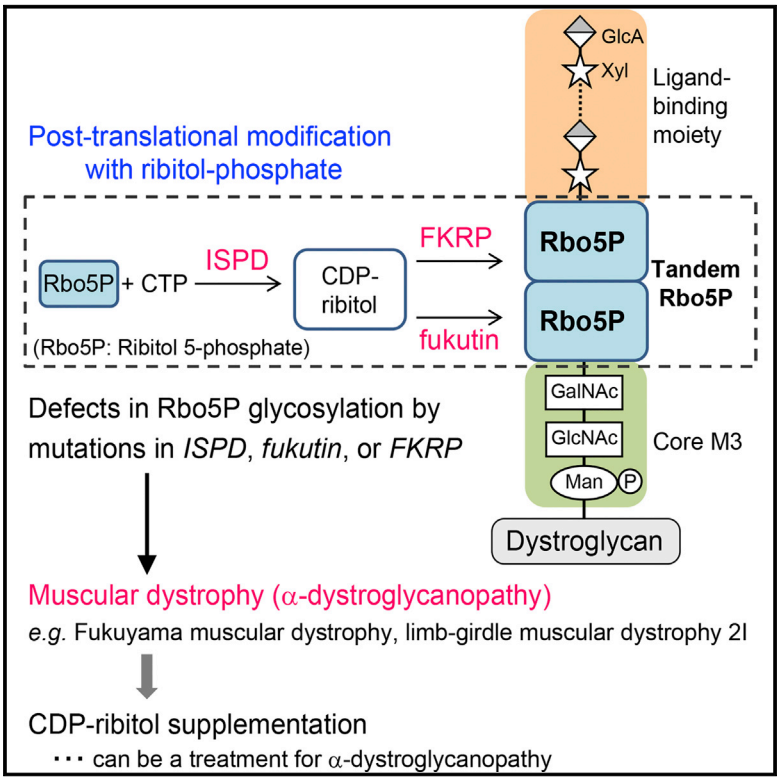

Highlights

- Ribitol 5-phosphate is a functional glycan unit in mammals
- α-dystroglycan function requires tandem ribitol 5-phosphate structure
- Muscular dystrophy proteins are involved in ribitol 5-phosphate glycosylation
- Supplementation with ribitol 5-phosphate metabolites may be a therapeutic strategy

Authors

Motoi Kanagawa, Kazuhiro Kobayashi, Michiko Tajiri, ..., Yoshinao Wada, Tamao Endo, Tatsushi Toda

Correspondence

waday@lab.mch.pref.osaka.jp (Y.W.), endo@tmig.or.jp (T.E.), toda@med.kobe-u.ac.jp (T.T.)

In Brief

Kanagawa et al. show that ribitol 5-phophate is a functional glycan unit in mammals and that defects in its post-translational modification pathway are associated with muscular dystrophy.

Kanagawa et al., 2016, Cell Reports *14*, 2209–2223
March 8, 2016 ©2016 The Authors
http://dx.doi.org/10.1016/j.celrep.2016.02.017

CellPress

Cell Reports
Article

OPEN ACCESS
CellPress

Identification of a Post-translational Modification with Ribitol-Phosphate and Its Defect in Muscular Dystrophy

Motoi Kanagawa,[1,7] Kazuhiro Kobayashi,[1,7] Michiko Tajiri,[2,7] Hiroshi Manya,[3,7] Atsushi Kuga,[1,7] Yoshiki Yamaguchi,[4] Keiko Akasaka-Manya,[3] Jun-ichi Furukawa,[5] Mamoru Mizuno,[6] Hiroko Kawakami,[6] Yasuro Shinohara,[5] Yoshinao Wada,[2,8,*] Tamao Endo,[3,8,*] and Tatsushi Toda[1,8,*]

[1]Division of Neurology/Molecular Brain Science, Kobe University Graduate School of Medicine, Kobe, Hyogo 650-0017, Japan
[2]Department of Molecular Medicine, Osaka Medical Center and Research Institute for Maternal and Child Health, Izumi, Osaka 594-1101, Japan
[3]Molecular Glycobiology, Research Team for Mechanism of Aging, Tokyo Metropolitan Geriatric Hospital and Institute of Gerontology, Itabashi, Tokyo 173-0015, Japan
[4]Structural Glycobiology Team, Systems Glycobiology Research Group, RIKEN-Max Planck Joint Research Center for Systems Chemical Biology, RIKEN Global Research Cluster, Wako, Saitama 351-0198, Japan
[5]Laboratory of Medical and Functional Glycomics, Graduate School of Advanced Life Science, and Frontier Research Center for Post-Genome Science and Technology, Hokkaido University, Sapporo, Hokkaido 001-0021, Japan
[6]Laboratory of Glyco-organic Chemistry, The Noguchi Institute, Itabashi, Tokyo 173-0003, Japan
[7]Co-first author
[8]Co-senior author
*Correspondence: waday@lab.mch.pref.osaka.jp (Y.W.), endo@tmig.or.jp (T.E.), toda@med.kobe-u.ac.jp (T.T.)
http://dx.doi.org/10.1016/j.celrep.2016.02.017
This is an open access article under the CC BY-NC-ND license (http://creativecommons.org/licenses/by-nc-nd/4.0/).

SUMMARY

Glycosylation is an essential post-translational modification that underlies many biological processes and diseases. α-dystroglycan (α-DG) is a receptor for matrix and synaptic proteins that causes muscular dystrophy and lissencephaly upon its abnormal glycosylation (α-dystroglycanopathies). Here we identify the glycan unit ribitol 5-phosphate (Rbo5P), a phosphoric ester of pentose alcohol, in α-DG. Rbo5P forms a tandem repeat and functions as a scaffold for the formation of the ligand-binding moiety. We show that enzyme activities of three major α-dystroglycanopathy-causing proteins are involved in the synthesis of tandem Rbo5P. Isoprenoid synthase domain-containing (ISPD) is cytidine diphosphate ribitol (CDP-Rbo) synthase. Fukutin and fukutin-related protein are sequentially acting Rbo5P transferases that use CDP-Rbo. Consequently, Rbo5P glycosylation is defective in α-dystroglycanopathy models. Supplementation of CDP-Rbo to *ISPD*-deficient cells restored α-DG glycosylation. These findings establish the molecular basis of mammalian Rbo5P glycosylation and provide insight into pathogenesis and therapeutic strategies in α-DG-associated diseases.

INTRODUCTION

α-dystroglycan (α-DG) was originally identified as a laminin receptor in the dystrophin-glycoprotein complex that is defective in Duchenne muscular dystrophy (Ibraghimov-Beskrovnaya et al., 1992). Subsequently, several matrix and synaptic proteins such as agrin, perlecan, and neurexin were identified as α-DG ligands (Yoshida-Moriguchi and Campbell, 2015). α-DG also functions as a receptor for Lassa virus (Cao et al., 1998). *O*-mannose (Man)-type glycosylation of α-DG is required for its ligand-binding activities, and abnormal glycosylation is associated with muscular dystrophy, lissencephaly, and cancer metastasis (Michele et al., 2002; Bao et al., 2009). Several genes have been identified to be responsible for α-dystroglycanopathy, a group of muscular dystrophies caused by aberrant α-DG glycosylation (Yoshida-Moriguchi and Campbell, 2015). α-dystroglycanopathy includes Fukuyama congenital muscular dystrophy (FCMD), muscle-eye-brain disease, Walker-Warburg syndrome, congenital muscular dystrophy (MDC) 1C/1D, and limb-girdle muscular dystrophy (LGMD) 2I. *Fukutin* is the causative gene for FCMD, and we have demonstrated that splicing-modulation therapy by antisense oligonucleotides is a promising clinical treatment for FCMD (Kobayashi et al., 1998; Taniguchi-Ikeda et al., 2011).

Some α-dystroglycanopathy gene products (POMGnT1, POMT1, and POMT2) are glycosyltransferases that synthesize the initially identified *O*-Man-type CoreM1 glycan [Galβ1,4GlcNAcβ1,2Man-] (Yoshida et al., 2001; Manya et al., 2004; Chiba et al., 1997). Recently, another *O*-Man glycan [GalNAcβ1,3GlcNAcβ1,4Man-], CoreM3, was identified in recombinant α-DG (Yoshida-Moriguchi et al., 2010), and several other α-dystroglycanopathy genes were also subsequently identified (Jae et al., 2013; Willer et al., 2012; Roscioli et al., 2012). The recently identified α-dystroglycanopathy genes *GTDC2* (*POMGNT2*) and *B3GALNT2* encode glycosyltransferases that synthesize the CoreM3 glycan (Yoshida-Moriguchi et al., 2013).

SGK196 (*POMK*) encodes a kinase that phosphorylates the C6 position of *O*-Man in CoreM3 (Yoshida-Moriguchi et al., 2013). The glycan structure directly involved in ligand binding is [-3Xylα1,3GlcAβ1-]$_n$ (hereafter referred to as the Xyl/GlcA repeat), which is synthesized by the glycosyltransferase LARGE (Inamori et al., 2012). It has been hypothesized that the Xyl/GlcA repeat branches from the phosphorylated *O*-Man in CoreM3 via a putative phosphodiester-linked moiety (Yoshida-Moriguchi et al., 2010). This is called a "post-phosphoryl moiety"; however, its structure is still unknown. In addition, the presence of α-dystroglycanopathy genes with unknown functions (*fukutin*, *FKRP*, *ISPD*, and *TMEM5*) suggests that an additional moiety and a synthetic pathway for α-DG maturation likely exist. To answer these questions and to better understand the pathogenesis of the α-dystroglycanopathies, we attempted to delineate the full functional glycan structure of α-DG.

RESULTS

Identification of Ribitol 5-Phosphate in the Sugar Chain of α-DG

For mass spectrometry (MS)-based structural analysis, we designed a small recombinant α-DG/Fc fusion protein, DGFc^{WT}, which contains the wild-type (WT) N-terminal domain and the first 20 amino acids of the mucin-like domain (from Ala314 to Pro333) (Figure 1A). Mature α-DG-Fc peptides begin with Gln311 because the N-terminal domain is processed during maturation (Kanagawa et al., 2004) and LARGE-dependent glycosylation takes place on the first two Thr residues in the mucin-like domain (Thr315 and Thr317) (Hara et al., 2011b). The results of western blotting using the IIH6 antibody, which recognizes the Xyl/GlcA repeat, and a laminin overlay assay suggested that DGFc^{WT} is modified with the Xyl/GlcA repeat and possesses laminin-binding activity in NIH 3T3 cells without LARGE overexpression (Figure 1B). To obtain glycopeptides that contain a functional moiety, we subjected the samples to an anion exchange column after removing the Fc tag, terminal sialic acids, and *O*-GalNAc-type glycans (Figure 1A). A stepwise elution with ammonium acetate (NH_4Ac) enabled us to fractionate the DGFc^{WT}-derived glycopeptides (DG^{WT}-GPs) according to the length of the negatively charged Xyl/GlcA repeat. MS of the fractions eluted with 0.5 M and 0.75 M NH_4Ac showed ladder peaks that differed from each other by 308.2 Da, which corresponded to the mass of a Xyl/GlcA unit (132.1 Da for Xyl and 176.1 Da for GlcA) (Figures 1C and 1D). The mass spectrum suggested the presence of at least 13 Xyl/GlcA repeats, which were sufficient for α-DG to bind laminin (Goddeeris et al., 2013). To expose the structure connecting the Xyl/GlcA repeat to *O*-Man glycan, we removed the Xyl/GlcA repeats by introducing a T190M missense mutation in the N-terminal domain; this mutation, identified in a patient with α-dystroglycanopathy, prevents LARGE-dependent glycosylation (Hara et al., 2011a) (Figure 1A). DGFc^{T190M} did not react with laminin or the IIH6 antibody (Figure 1B). In contrast to DG^{WT}-GPs, DG^{T190M}-GPs from the 0.5 M NH_4Ac eluate did not have the 308 Da repeats and instead contained a GP of 6,138 Da (*m/z* 6,139.1; GP6138) and an unglycosylated peptide (3,536 Da; *m/z* 3,537.1) (Figure 1E). Furthermore, the mass spectrum of DG^{WT}-GPs from the 0.5 M NH_4Ac eluate suggested that the Xyl/GlcA repeat stemmed from GP6138 (6,139.1 plus a Xyl/GlcA unit corresponded to the first ladder signal at 6,447.4) (Figures 1C and 1E). Indeed, LARGE added the Xyl/GlcA repeat to GP6138 from DG^{T190M}-GPs in vitro (Figure S1), indicating that GP6138 contains the core acceptor structure for LARGE-dependent modifications.

It has been conceived that the Xyl/GlcA modification requires a phosphodiester-linked structure (Yoshida-Moriguchi et al., 2013). To identify the phosphodiester-linked structure, DG^{WT}-GPs from the 0.75 M NH_4Ac eluate were treated with hydrofluoric acid (HF), which cleaves the phosphodiester linkage of α-DG (Yoshida-Moriguchi et al., 2010) and DGFc proteins, resulting in a loss of IIH6 reactivity (Figure 1F). After treatment, the peaks in the high mass region converged into two major ions at *m/z* 5,402.7 and *m/z* 5,322.7 (Figure 1G), of which the mass of the former ion corresponded well to the GP containing one phosphorylated CoreM3 glycan (Yoshida-Moriguchi et al., 2010), two CoreM1 glycans (Chiba et al., 1997), and one hexose moiety (Figure 2A, green background). The ion at *m/z* 5,322.7 corresponds to the same GP that lacks a phosphate. These results suggest that GP6138 contains a phosphodiester-linked structure of 736.5 Da (6,139.1 minus 5,402.7; hereafter, we describe this moiety as "Structure736") (Figure 2A, blue background). To identify the components of Structure736, we treated the GP6138-rich fractions from the DG^{T190M}-GPs with HF and then subjected the ions in the low mass region to MS/MS. The MS/MS spectrum suggests that Structure736 contains a terminal Xyl/GlcA unit and an alternating repeat of 80 Da and 134 Da (Figures S2A–S2D). The high resolving power MS elucidated the precise mass of the 134 Da component to be 134.05787 or 134.05791, specifying the elemental composition as $C_5H_{10}O_4$ (134.05791 Da for theoretical mass) (Figure 2B). Similarly, the 80 Da moiety was identified as PO_3H (79.96633) rather than SO_3 (79.95682) (Figure 2B).

To more easily enable tandem MS for the GPs, we constructed a mutant, DGFc^{T320K}, which results in a small peptide following lysylendopeptidase (LEP) digestion (Figure 1A). This DGFc mutant was properly modified with the laminin-binding glycan (Figure 1B). We prepared DG^{T320K}-GP of 2,986 Da (GP2986), which corresponds to a glycopeptide (QIHATPTPVK) with one phosphorylated CoreM3, one CoreM1, and Structure736, and then subjected it to MS/MS. The results confirmed that GP2986 contains the 80 Da and 134 Da repeat, which is linked to the terminal Xyl/GlcA unit and the core HexNAc-HexNAc at each end (Figure S2E). More intriguingly, the presence of the product ion at *m/z* 1,452.2 from the precursor indicates that Structure736 is not attached to the phosphate of the innermost *O*-Man residue.

There were three candidate residues with the chemical formula $C_5H_{12}O_5$ (hydrated $C_5H_{10}O_4$): xylitol, D/L-arabitol, and ribitol (Rbo). However, mammalian cells are not known to utilize these compounds for post-translational modifications. Interestingly, microorganisms, such as Gram-positive bacteria, use a repeating unit of ribitol 5-phosphate (Rbo5P), which forms a phosphodiester-linked polyol structure, teichoic acid, as a major cell wall component (Brown et al., 2013). We hence performed composition analysis of DGFc^{T190M} using gas chromatography (GC)-MS and detected three peaks (Gp1, Gp2, and Gp3) with

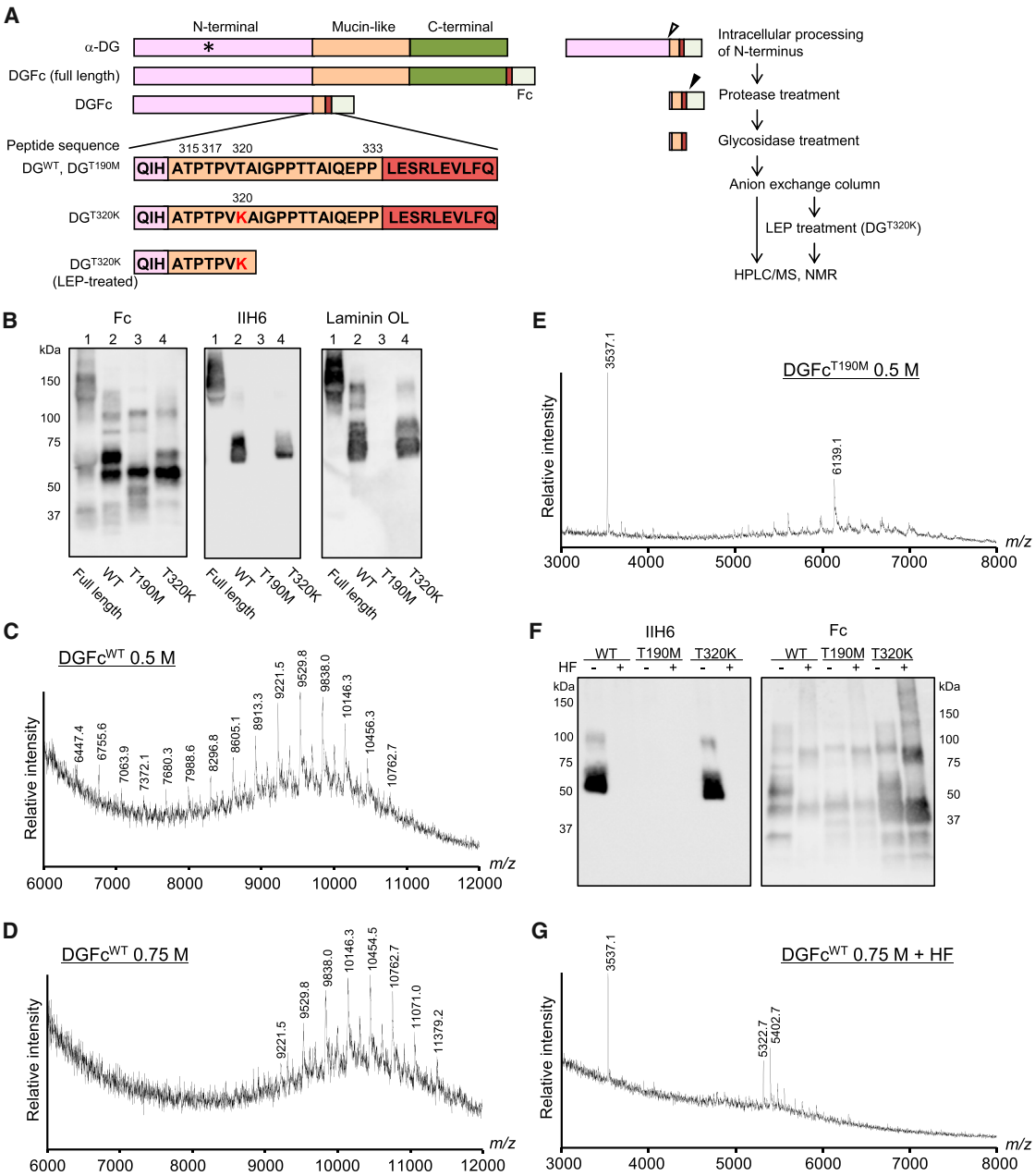

Figure 1. Characterization of the DGFc Proteins

(A) Schematic representation of the α-DG constructs and their amino acid sequences. Mouse α-DG is composed of N-terminal, mucin-like, and C-terminal domains. A protease cleavage site was inserted between the α-DG and Fc portions (brown). The asterisk indicates the missense T190M mutation. (Right) Scheme for purification of the glycopeptides.

(B) Western blot analysis and laminin overlay assay of the DGFc proteins. DGFc (full-length), $DGFc^{WT}$, $DGFc^{T190M}$, and $DGFc^{T320K}$ were subjected to western blotting with a biotinylated anti-Fc antibody, IIH6 antibody, and to the laminin overlay assay.

(C–E) MALDI mass spectra of DGFc-derived glycopeptides. (C) DG^{WT}-GP (0.5 M NH_4Ac). (D) DG^{WT}-GP (0.75 M NH_4Ac). (E) DG^{T190M}-GP (0.5 M NH_4Ac).

(F) HF treatment of the DGFc proteins. $DGFc^{WT}$, $DGFc^{T190M}$, and $DGFc^{T320K}$ with (+) or without (–) HF treatment were analyzed by western blotting with IIH6 and anti-Fc antibodies.

(G) MALDI mass spectra of HF-treated DG^{WT}-GP (0.75 M NH_4Ac).

See also Figure S1.

similar retention times as the standard Rbo5P (Rp1, Rp2, and Rp3) (Figure 3A). The mass spectra of these peaks are highly matched to those of species with the structural formulas of anhydrous acetylated Rbo and acetylated Rbo (Figure 3B). We also confirmed that this GC analysis is able to distinguish Rbo from xylitol and arabitol (data not shown). These data indicate that

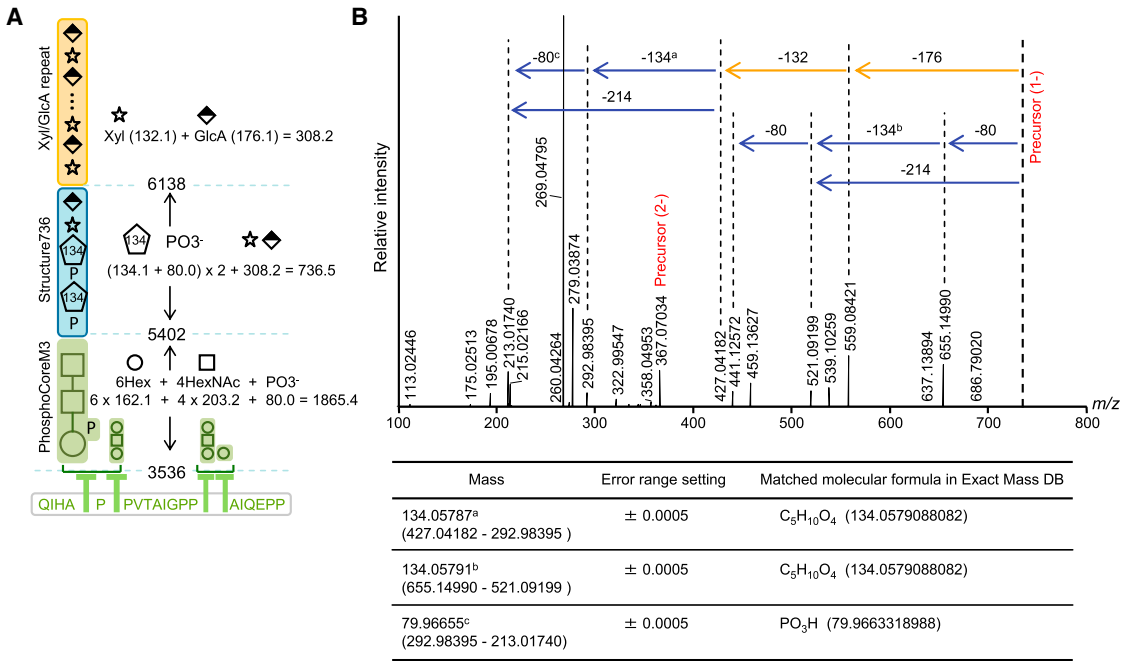

Mass	Error range setting	Matched molecular formula in Exact Mass DB
134.05787[a] (427.04182 - 292.98395)	± 0.0005	$C_5H_{10}O_4$ (134.0579088082)
134.05791[b] (655.14990 - 521.09199)	± 0.0005	$C_5H_{10}O_4$ (134.0579088082)
79.96655[c] (292.98395 - 213.01740)	± 0.0005	PO_3H (79.9663318988)

Figure 2. High-Resolution MS Analysis of α-DG

(A) Schematic representation of the sugar components of DG-GP; Structure736 (blue), the CoreM3 glycan (green), and the Xyl/GlcA repeat (orange).

(B) High-resolution MS. The product ion mass spectrum from the precursors at *m/z* 367 for double charge or *m/z* 735 for single charge suggests that Structure736 contains a Xyl/GlcA unit (orange arrows) and moieties consisting of 80 Da and 134 Da (blue arrows). The fragments of the 134 Da and 80 Da moieties (indicated by a, b, and c) were cross-referenced to the exact mass database, and the results are shown in the table.

See also Figure S2.

DGFc^{T190M} contains Rbo residues and that the moiety consisting of 80 Da and 134 Da structures is Rbo phosphate (RboP).

ISPD Is a CDP-Ribitol Synthase

In Gram-positive bacteria, the Rbo5P polymer is synthesized by the TarK and TarL enzymes (Tar; Teichoic acid ribitol), which use CDP-Rbo as a donor substrate, and CDP-Rbo is synthesized by the TarI enzyme from cytidine triphosphate (CTP) and Rbo5P (Brown et al., 2013). We found that bacterial TarI shared homology with mammal ISPD, which is one of the causative gene products for α-dystroglycanopathy (Figure S3A) (Willer et al., 2012; Roscioli et al., 2012). To determine whether ISPD possesses CDP-Rbo synthase activity, we prepared His-tagged human ISPD, incubated it with CTP and Rbo5P, and then analyzed the products by high-performance liquid chromatography (HPLC). After the reaction of ISPD with both Rbo5P and CTP, a novel peak was detected (Figure 4A, indicated by "P"), and the same peak was observed in the TarI enzyme products (Figure S3B). MS results of both products showed the same mass of 537 Da, which was compatible with CDP-Rbo (Figures 4B and S3C). Thus, the enzymatic properties of human ISPD were identical to those of bacterial TarI. Pathogenic mutations of the *ISPD* gene impaired CDP-Rbo synthesizing activity (Figures 4C and S3A). These data indicate that ISPD is a mammalian CDP-Rbo synthase.

Fukutin and FKRP Are Ribitol 5-Phosphate Transferases

The fukutin family is predicted to encode a phosphoryl-ligand transferase (Aravind and Koonin, 1999; Kuchta et al., 2009). *Fukutin-related protein* (*FKRP*) was originally identified as a causative gene for MDC1C/LGMD2I based on its sequence homology with *fukutin* (Brockington et al., 2001a). Both fukutin and FKRP proteins contain the putative catalytic DXD motif, which is a conserved motif found in many families of glycosyltransferases (Wiggins and Munro, 1998; Tachikawa et al., 2012; Esapa et al., 2002). Therefore, we examined whether fukutin and FKRP are involved in RboP modification. A synthetic peptide mimicking mouse α-DG (ATPAPVAAIGPK) was enzymatically modified with phosphorylated CoreM3 (phosphoCoreM3-peptide) (see Supplemental Experimental Procedures) and then used as an acceptor substrate. Fukutin and FKRP were prepared as secreted proteins with a His/myc-tag at the N terminus (s-fukutin and sFKRP, respectively). First, we incubated s-fukutin with CDP-Rbo and phosphoCoreM3-peptide and then conducted HPLC and MS analyses. A novel peak was detected in the presence of s-fukutin (Figure 5A, indicated as "P1"), and this product showed an increase in 214 Da (compatible with a RboP) from phosphoCoreM3-peptide (1,997.0 minus 1,782.9; Figure 5B). These data indicate that s-fukutin transfers Rbo5P from CDP-Rbo to phosphoCoreM3-peptide. Missense mutations found in FCMD patients and in the putative catalytic sites reduced s-fukutin enzyme activity (Figures 5C and S4A).

To examine whether FKRP also has Rbo5P transferase activity, we incubated sFKRP with CDP-Rbo and either phosphoCoreM3-peptide or Rbo5P-phosphoCoreM3-peptide. Although sFKRP did not react with phosphoCoreM3-peptide, its reaction with Rbo5P-phosphoCoreM3-peptide produced a

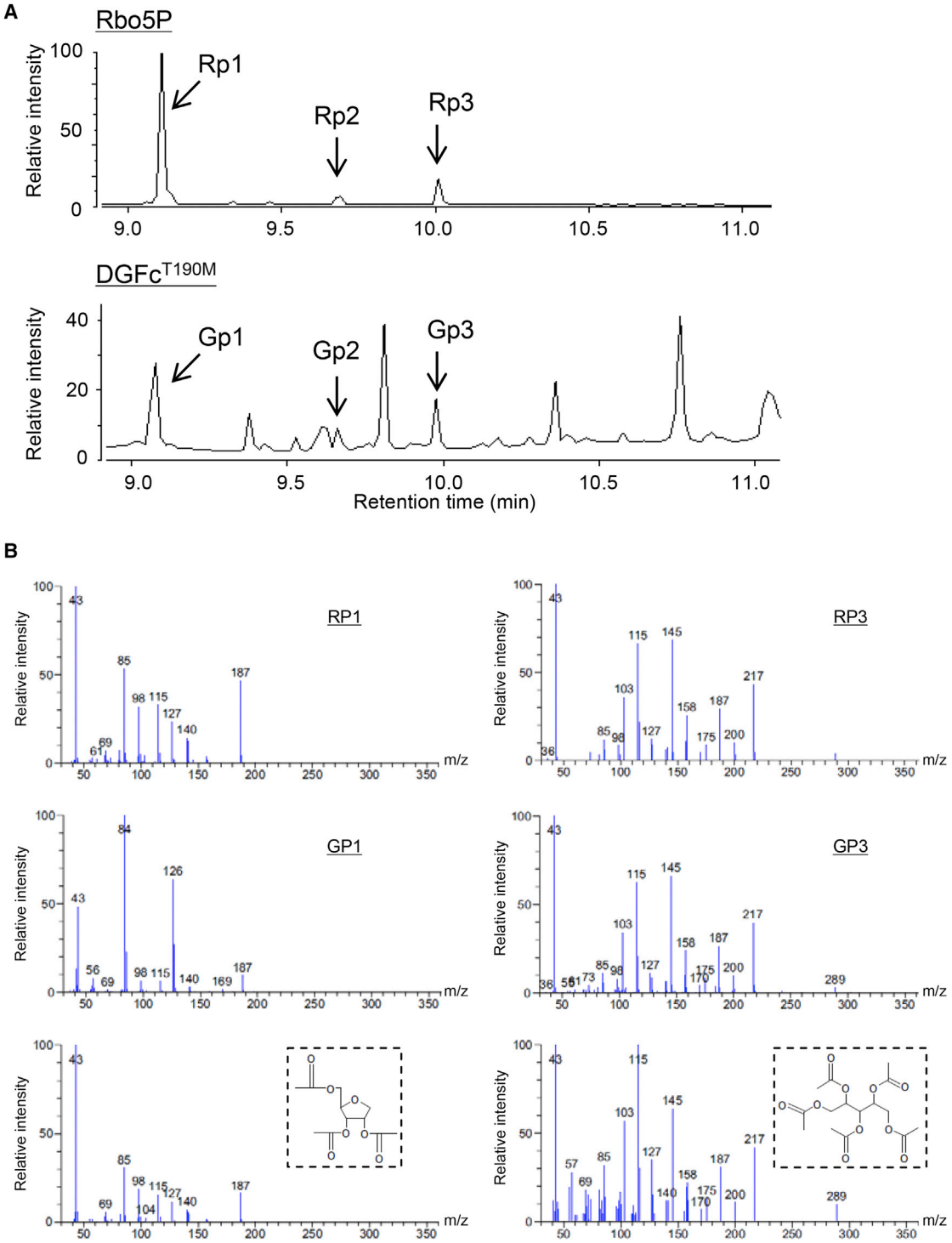

Figure 3. Identification of Ribitol-Phosphate in α-DG

(A) Gas chromatogram of the alditol acetate derivatives of Rbo5P (top) and DGFc^{T190M} (bottom). The Rp1, Rp2, and Rp3 peaks correspond with those of Gp1, Gp2, and Gp3, respectively.

(B) GC-MS of Rbo5P and DGFc^{T190M}. The Rp1, Gp1, Rp3, and Gp3 peaks shown in (A) were analyzed by MS. The mass spectra of these peaks were cross-referenced to the NIST database. The matched spectra with structural formulas are shown in the bottom panels.

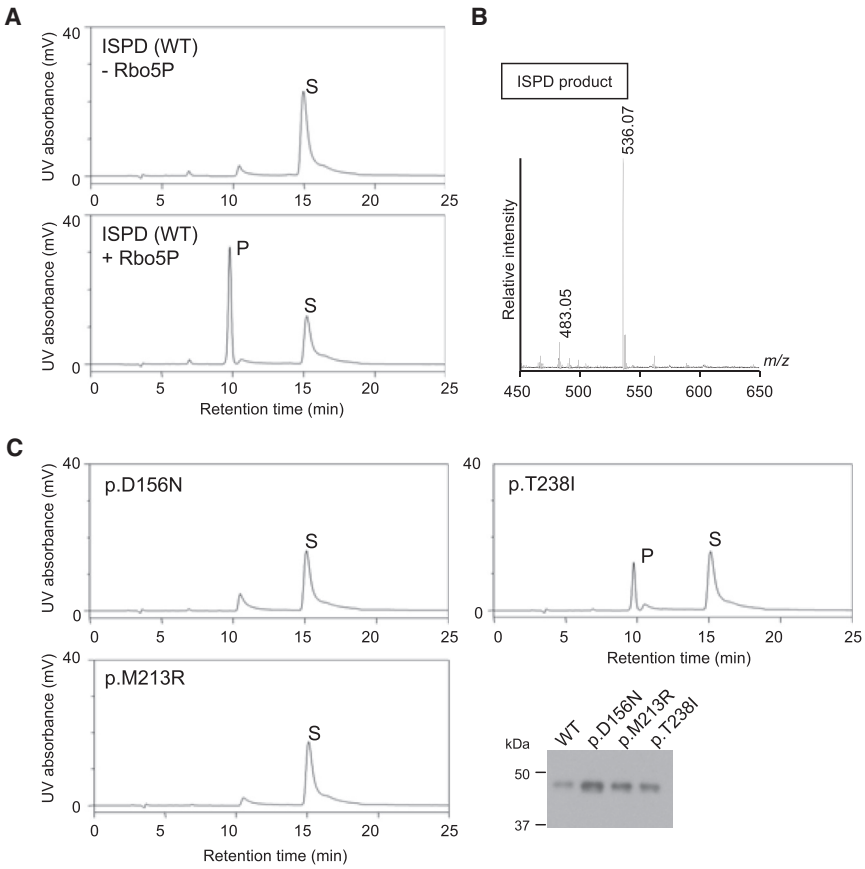

Figure 4. ISPD Is a CDP-Rbo Synthase

(A and B) Enzymatic activity of human ISPD. ISPD enzyme reactions were performed with or without Rbo5P, and the products were analyzed by HPLC. S, unreacted acceptor substrate. P, enzyme product. The fraction including the reaction products (the peak designated as P in A) was analyzed by MS in the negative ion mode (B).

(C) Enzyme activities of the ISPD mutants. Quantities of the mutant proteins were confirmed to be comparable by western blotting.

See also Figure S3.

novel peak (Figure 5D, indicated as "P2") and the product showed an increase in mass of 214 Da (2,211.1 minus 1,997.0; Figures 5B and 5E). These data indicate that sFKRP transfers the second Rbo5P to the s-fukutin products. Missense mutations found in α-dystroglycanopathy patients and in the putative catalytic sites reduced sFKRP enzyme activity (Figures 5F and S4A). Finally, we fractionated mouse liver membrane preparations and performed fukutin and FKRP enzyme assays (Figure S4B). The distributions of both enzyme activities were similar to the distribution of a Golgi marker protein, which suggest that fukutin and FKRP activities reside in the Golgi apparatus.

Determination of the Tandem Ribitol Structure

To determine the precise structure of the fukutin-dependent moiety, we conducted large-scale preparation of s-fukutin products using the acceptor substrate GalNAcβ1,3GlcNAcβ-pNp (pNp, *p*-nitrophenyl). We confirmed that s-fukutin can transfer Rbo5P to GalNAcβ1,3GlcNAcβ-pNp (Figures S4C and S4D). The original acceptor substrate (GalNAcβ1,3GlcNAcβ-pNp) and the purified s-fukutin product were analyzed by a series of NMR measurements, including ^{1}H-^{13}C heteronuclear single quantum correlation (HSQC) and 2D ^{1}H-^{31}P heteronuclear multiple-bond correlation (HMBC). In the ^{1}H-^{13}C HSQC spectra, a ^{13}C downfield shift (~4 ppm) was observed at the GalNAc C3 position after the s-fukutin reaction (Figures 6A and S5A). Importantly, a through-bond ^{1}H-^{31}P correlation was observed in the s-fukutin product between the phosphorus and GalNAc H3 (Figure 6A). Thus, Rbo5P is linked to the C3 position of GalNAc via a phosphodiester linkage (Rbo5P-3GalNAc). Therefore, fukutin is an enzyme that transfers Rbo5P from CDP-Rbo to the C3 position of GalNAc in the CoreM3 glycan (CDP-Rbo: GalNAc-3 Rbo5P transferase).

To determine the precise structure of the FKRP-dependent moiety, we performed large-scale preparation of sFKRP products from Rbo5P-3GalNAcβ1,3GlcNAcβ-pNp (Figures S4E and S4F), and analyzed them by ^{1}H-^{13}C HSQC and 2D ^{1}H-^{31}P HMBC experiments. In the ^{1}H-^{13}C HSQC spectra, significant chemical shift changes were observed for the signals originating from the first Rbo5P residue (Rbo-C1 in Glycan2 and Glycan3), and additional peaks were detected from the second Rbo residue (Rbo'; Figures 6B and S5A). Furthermore, a through-bond ^{1}H-^{31}P correlation was observed in the sFKRP product between the phosphorus of the second Rbo5P residue (Rbo'5P) and the H1 of the first Rbo5P residue (Figure 6B). These NMR data revealed that the second Rbo (Rbo') is attached to the C1 position of the first Rbo residue via a phosphodiester linkage (Figures 6B and S5A). Therefore, FKRP is an enzyme that transfers the Rbo5P from CDP-Rbo to the C1 position of the first Rbo5P (CDP-Rbo: Rbo5P-1 Rbo5P transferase).

We further analyzed the Rbo5P-modified products that were enzymatically synthesized, by 1D ^{31}P NMR analysis (Figure 6C). PhosphoCoreM3-peptide showed a signal originating from Man-6-phosphate (Man6P). A peak at −3 ppm was observed in both Rbo5P-3GalNAcβ1,3GlcNAcβ-pNp and Rbo5P-phosphoCoreM3-peptide, which was assigned to the phosphorous of the first Rbo5P residue. The products of the sFKRP reaction (Rbo'5P-1Rbo5P-3GalNAcβ1,3GlcNAcβ-pNp and Rbo'5P-1Rbo5P-phosphoCoreM3-peptide) showed an additional peak (−2 ppm), which was assigned to the phosphorous from the second Rbo5P (Rbo'5P). The 1D ^{31}P spectrum of purified DG^{T190M}-GP6138 showed three signals, likely originating from Man6P, the first Rbo5P, and the second

Rbo5P (Rbo'5P). Thus, the tandem Rbo5P moiety is present in the α-DG protein expressed in mammalian cells. Finally, to corroborate that the tandem Rbo5P is not modified on the Man6P residue in the CoreM3 glycan, we analyzed the s-fukutin and sFKRP products from phosphoCoreM3-peptide by NMR (Figures S5B–S5D). The GalNAc-C3 and Rbo-C1 signals showed significant chemical shift changes after the s-fukutin and sFKRP reactions, respectively; however, the chemical shift of the Man-C6 signal did not change after the reactions. These observations support that the tandem Rbo5P moiety extends from the GalNAc residue, and not from the Man residue, in the CoreM3 glycan (Figure 6D).

Defects of Ribitol 5-Phosphate Glycosylation in α-Dystroglycanopathy Models and Potential Therapeutic Strategies

To examine whether Rbo5P glycosylation is affected in α-dystroglycanopathy, we generated HAP1 cells with a disruption in *ISPD*, *fukutin*, or *FKRP* genes as disease models, by CRISPR/Cas9 gene editing (Figure S6). We confirmed the disruption of functional α-DG glycosylation in these cells by western blot analysis using the IIH6 antibody. Rescue experiments confirmed that the abnormal glycosylation was caused by a loss of the targeted genes. We first expressed $DGFc^{WT}$ in normal HAP1 cells and analyzed DG^{WT}-GPs from the 0.25 M and 0.5 M NH_4Ac eluates by MS (Figures 7A and 7B). The data indicated the presence of ions containing Structure736 in the DG^{WT}-GP preparations and that the Xyl/GlcA units were modified on these GPs (Figure 7B). We then performed MS analyses on DG^{WT}-GPs prepared from the HAP1 cells with each α-dystroglycanopathy gene defect. Although the ions containing the phosphorylated CoreM3 glycan were detected in the *ISPD*- or *fukutin*-disrupted cells, no signals were assigned to GPs containing the Rbo5P moiety (Figures 7C and 7D). These data indicate that DG^{WT}-GPs prepared from *ISPD*- or *fukutin*-disrupted HAP1 cells lacked Structure736 and also support the idea that fukutin acts as a priming enzyme for Rbo5P modification. In the *FKRP*-disrupted cells, GPs containing a portion of Strucuture736 (single Rbo5P, 214 Da) were observed (Figure 7E), which supports the idea that FKRP synthesizes the second Rbo5P in the tandem structure. Taken together, these results confirmed that ISPD, fukutin, and FKRP are required for the synthesis of the tandem Rbo5P structure and indicate that Rbo5P glycosylation defects cause the loss of functional glycosylation of α-DG, resulting in α-dystroglycanopathy.

Our data also suggest that formation of the tandem Rbo5P structure requires CDP-Rbo and that *ISPD*-deficient α-dystroglycanopathy is caused by a lack of cellular CDP-Rbo. To examine whether supplementation of CDP-Rbo restores the functional glycosylation of α-DG, we treated *ISPD*-deficient HAP1 or HEK293 cells with exogenous CDP-Rbo (Figure 7F). The addition of CDP-Rbo to the cell culture medium restored the functional glycosylation of α-DG. In HEK293 cells, pretreatment of CDP-Rbo with a transfection reagent increased the efficacy of the restoration of α-DG glycosylation. These results raise the possibility of CDP-Rbo supplementation as a treatment for α-dystroglycanopathy patients.

DISCUSSION

Our data demonstrate that tandem Rbo5P is a "post-phosphoryl moiety." The structure required for the functional maturation of α-DG was determined to be "Rbo5P-1Rbo5P-3GalNAcβ1,3GlcNAcβ1,4Man(6P)-*O*" (Figure 6D). Post-phosphoryl modifications, including LARGE-dependent Xyl/GlcA repeats, have been thought to extend from phosphorylated Man (Yoshida-Moriguchi et al., 2010); however, our present data indicate that the monoester-linked phosphate on the C6-position of *O*-Man exists independently of the HF-sensitive Rbo5P tandem structure and that the Xyl/GlcA repeats extend from the tandem Rbo5P. We speculate that mannosyl phosphorylation determines the substrate specificity of Rbo5P and/or Xyl/GlcA modifications. Recently, B4GAT1 was shown to be a GlcA transferase, which synthesizes an acceptor primer necessary for LARGE-dependent Xyl/GlcA repeat formation (Praissman et al., 2014; Willer et al., 2014). Structure736 contains a LARGE-independent Xyl/GlcA unit, which can be elongated by LARGE activity (Figures 2 and S1). These data also confirm that the Rbo5P tandem structure is a central part of the post-phosphoryl moiety and is required for the functions of α-DG.

We subsequently identified the activities of three α-dystroglycanopathy-causing proteins, namely, ISPD, fukutin, and FKRP, to be involved in Rbo5P glycosylation (Figure 6D). ISPD is a CDP-Rbo synthase that uses Rbo5P and CTP. This finding suggests that cellular levels of Rbo5P and CTP may control the Rbo5P modification of α-DG. In bacteria, Rbo5P is synthesized by the TarJ enzyme from ribulose 5-phosphate and nicotinamide adenine dinucleotide phosphate (Brown et al., 2013). In mammals, however, neither the ortholog of TarJ nor the biosynthetic pathway of Rbo5P is currently known. It is hence important in the future to identify proteins that are involved in mammalian Rbo5P biosynthesis, because they may regulate the functional glycosylation of α-DG and thus may cause α-dystroglycanopathy upon their mutations.

Fukutin and FKRP are both Rbo5P transferases that use CDP-Rbo as a common donor substrate. On the other hand, the selectivity of fukutin and FKRP for acceptor substrates showed a distinct difference: FKRP and fukutin are not able to transfer Rbo5P to GalNAc and to the first Rbo5P residue, respectively. Thus, formation of the tandem Rbo5P structure likely needs to be performed in a sequential manner. In addition, we have not observed polymer formation of more than two Rbo5P residues by the activities of fukutin or FKRP. These data suggest the existence of strict mechanisms that determine substrate specificity or regulate the formation of the tandem RboP structure. It is unknown whether negative regulatory factors of the tandem Rbo5P structure exist, for example, phosphodiesterase-like activities that cleave the internal phosphodiester linkage of the Rbo5P tandem structure. If such activities exist, they may be able to regulate the functional glycosylation of α-DG, and the elevated expression or hyperactivation of such enzymes may result in the abnormal glycosylation of α-DG.

Several studies have suggested the Golgi localization of fukutin and FKRP based on the localization of exogenously expressed proteins (Kobayashi et al., 1998; Esapa et al., 2002). Our fractionation and enzyme assays also suggest that

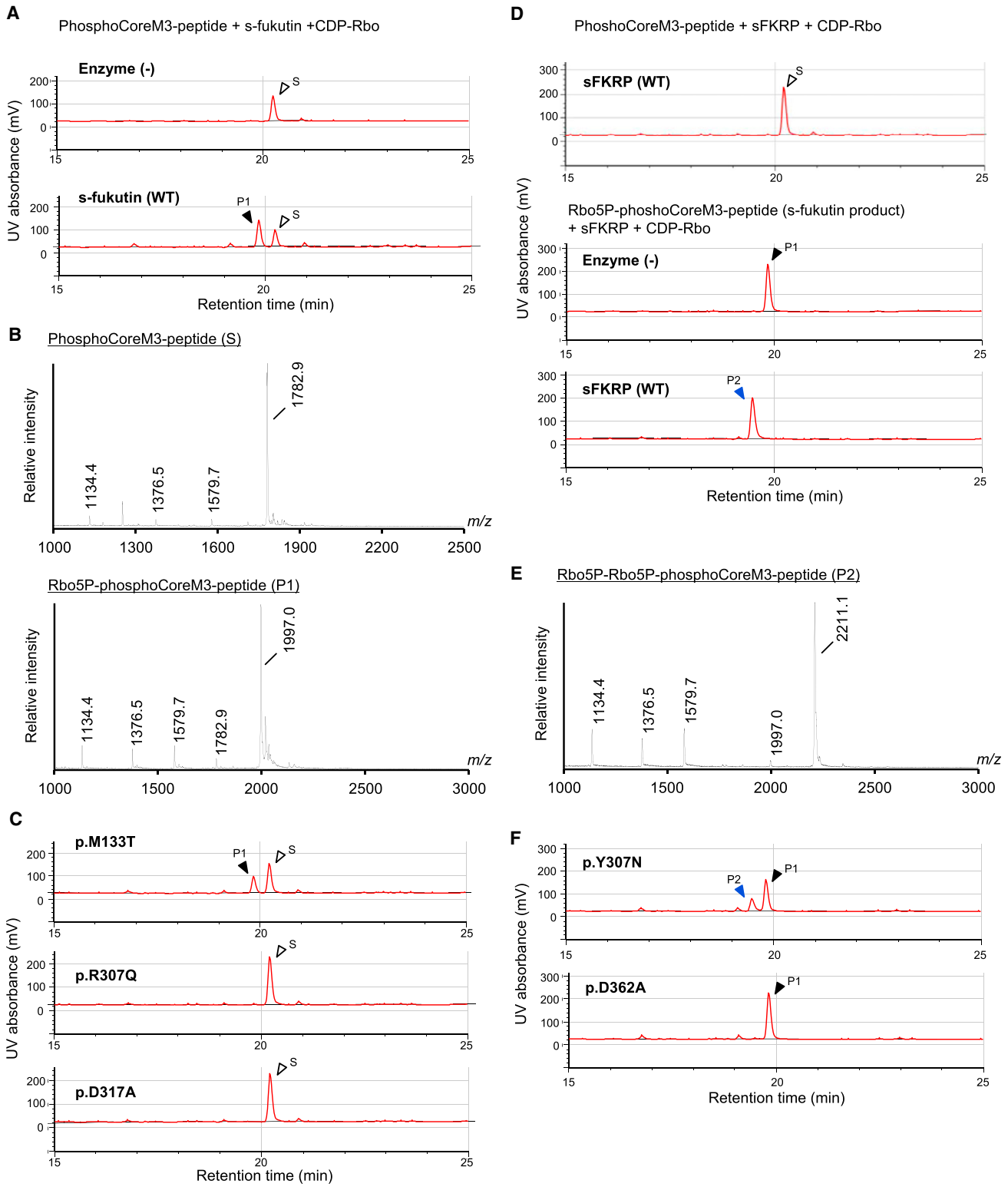

Figure 5. Fukutin and FKRP Are Rbo5P Transferases

(A and B) Enzyme reaction of fukutin. PhosphoCoreM3-peptide was used as an acceptor substrate for s-fukutin. S, unreacted acceptor substrate. P1, s-fukutin enzyme product. PhosphoCoreM3-peptide and the fraction containing the s-fukutin products (S and P1 in A) were analyzed by MS in the negative ion mode (B). (C) The activities of s-fukutin with disease-causing mutations (p.M133T and p.R307Q) and with a mutation in the putative catalytic sites (p.D317A).

(legend continued on next page)

endogenous fukutin and FKRP activities are localized in the Golgi. Given that the LARGE-dependent Xyl/GlcA repeat is also synthesized in the Golgi (Yoshida-Moriguchi et al., 2013), we propose that the Rbo5P modification occurs in the Golgi apparatus. We showed that some disease-causing missense mutations in fukutin or FKRP proteins directly reduced their enzyme activity, but the mislocalization of these proteins containing disease-causing missense mutations has been also reported (Esapa et al., 2002; Tachikawa et al., 2012). A protein motif search and deglycosylation experiments suggested that both fukutin and FKRP are *N*-glycosylated proteins (data not shown). Mutations in their potential glycosylation sites may cause α-dystroglycanopathy by altering the cellular localization of or the protein stability of fukutin and FKRP. Indeed, a missense mutation in the potential glycosylation site of FKRP (p.S174C) has been reported (Quijano-Roy et al., 2006).

Recent studies reported that *ISPD* mutations are a relatively common cause of α-dystroglycanopathy (Willer et al., 2012; Roscioli et al., 2012; Cirak et al., 2013). In Japan, most cases of α-dystroglycanopathy are confirmed to be FCMD, which is caused by mutations in *fukutin* (Kobayashi et al., 1998; Matsumoto et al., 2005). LGMD2I, which is caused by mutations in *FKRP*, is a common form of LGMD in western countries (Brockington et al., 2001b). Taken together, a substantial proportion of α-dystroglycanopathy is caused by abnormalities in the Rbo5P glycosylation pathway. Although 18 genes are currently known to cause abnormal glycosylation of α-DG upon their mutation, resulting in α-dystroglycanopathy (Yoshida-Moriguchi and Campbell, 2015), the causative genes for a proportion of α-dystroglycanopathy cases still remain to be identified. Some of the as-yet-unidentified causative genes of α-dystroglycanopathy may function in the Rbo5P glycosylation pathway, including CDP-Rbo biosynthesis. Clarifying the Rbo5P glycosylation pathway may accelerate our understanding of the pathogenesis of α-dystroglycanopathy.

We showed that the addition of CDP-Rbo restored the functional glycosylation of α-DG in *ISPD*-deficient cells, which indicates that metabolic components such as Rbo5P and CDP-Rbo in the Rbo5P glycosylation pathway can be targets of molecular supplementation therapy for α-dystroglycanopathy. Although the glycosylation pattern of α-DG varies among different cells and tissues, the IIH6-sensitive functional glycan is present in many cells and tissues (Kuga et al., 2012). α-DG in HEK293 and HAP cells contains functional glycans, and gene editing and rescue experiments validated their suitability for their use as disease model cells; however, further studies using animal models will be necessary for the development of CDP-ribitol supplementation therapy. Several lines of evidence have established that abnormal glycosylation of α-DG contributes to the invasive and proliferative phenotypes of cancer cells (Singh et al., 2004; Bao et al., 2009; Miller et al., 2015). Recently, an association between the downregulation of *ISPD* and mortality in clear cell renal cell carcinoma was reported (Miller et al., 2015). Thus, our findings suggest the involvement of the Rbo5P glycosylation pathway in tumor formation, as well as the possibility of molecular CDP-Rbo supplementation as a therapy for cancers.

Because Rbo5P has only been found in bacteria (Brown et al., 2013) and some plants such as *Adonis vernalis* (Negm and Marlow, 1985), it is surprising that mammalian cells use Rbo5P as a functional component of post-translational modifications. Rbo5P is a component of the teichoic acids in bacterial cell walls, which play various roles in bacterial physiology such as cell shape determination, cell division, and host defenses (Brown et al., 2013). How vertebrates acquired the Rbo5P modification during evolution, including the possibility of its horizontal transmission, would be interesting to investigate. As for its physiological functions, Rbo5P glycosylation is expected to be involved in many biological processes, such as embryonic and postnatal tissue development, as demonstrated by studies using *fukutin* and *FKRP* transgenic animals (Kurahashi et al., 2005; Ackroyd et al., 2009; Kanagawa et al., 2013). An intriguing question arises as to whether Rbo5P-containing glycoconjugates other than α-DG also exist. Given that DG-deficient mice recapitulate aspects of fukutin- or FKRP-deficient α-dystroglycanopathies (Moore et al., 2002; Cohn et al., 2002), α-DG is thought to be a primary target of Rbo5P modification. We cannot exclude the possibility of the existence of a Rbo5P transferase other than fukutin and FKRP, as well as that of a Rbo5P-containing glycoprotein or glycolipid other than α-DG. Investigating these possibilities will lead to a deeper understanding of Rbo5P modifications.

The complexity of the glycosylation machinery and the possible existence of unidentified sugar units may hinder our understanding of glycosylation-dependent biological processes and the pathogenesis of human diseases. We propose that Rbo5P glycosylation is an essential modification in mammals and that defects in the Rbo5P glycosylation pathway underlie the pathogenesis of muscular dystrophy and possibly of cancer metastasis and virus infection. Together, our results expand our knowledge on post-translational modification and establish an additional disease mechanism.

EXPERIMENTAL PROCEDURES

Glycopeptide Purification from the DGFc Proteins

DGFc proteins were secreted into the cell culture media and recovered with Protein A-beads. The DGFc proteins were eluted with 0.1 M glycine-HCl (pH 2.5) and then neutralized with a final concentration of 0.2 M Tris-HCl (pH 8.0). PreScission protease treatment to cleave the Fc tag was performed according to the manufacturer's instructions (GE Healthcare Life Science). The cleaved Fc tag and the protease were removed by Protein A-beads and glutathione beads, respectively. The samples were desalted using a Zeba spin column (Life Technologies) and then freeze-dried. The freeze-dried samples were dissolved with 20 mM phosphate buffer (pH 7.0) and treated

(D and E) Enzyme reaction of FKRP. Either PhosphoCoreM3-peptide (upper panel) or the s-fukutin product (P1, lower panels) was used as an acceptor substrate for sFKRP. P1, unreacted acceptor substrate (s-fukutin product). P2, sFKRP enzyme product. The fraction containing the sFKRP products (P2 in D) was analyzed by MS in the negative ion mode (E).

(F) The activities of sFKRP with a disease-causing mutation (p.Y307N) and with a mutation in the putative catalytic site (p.D362A).

See also Figure S4.

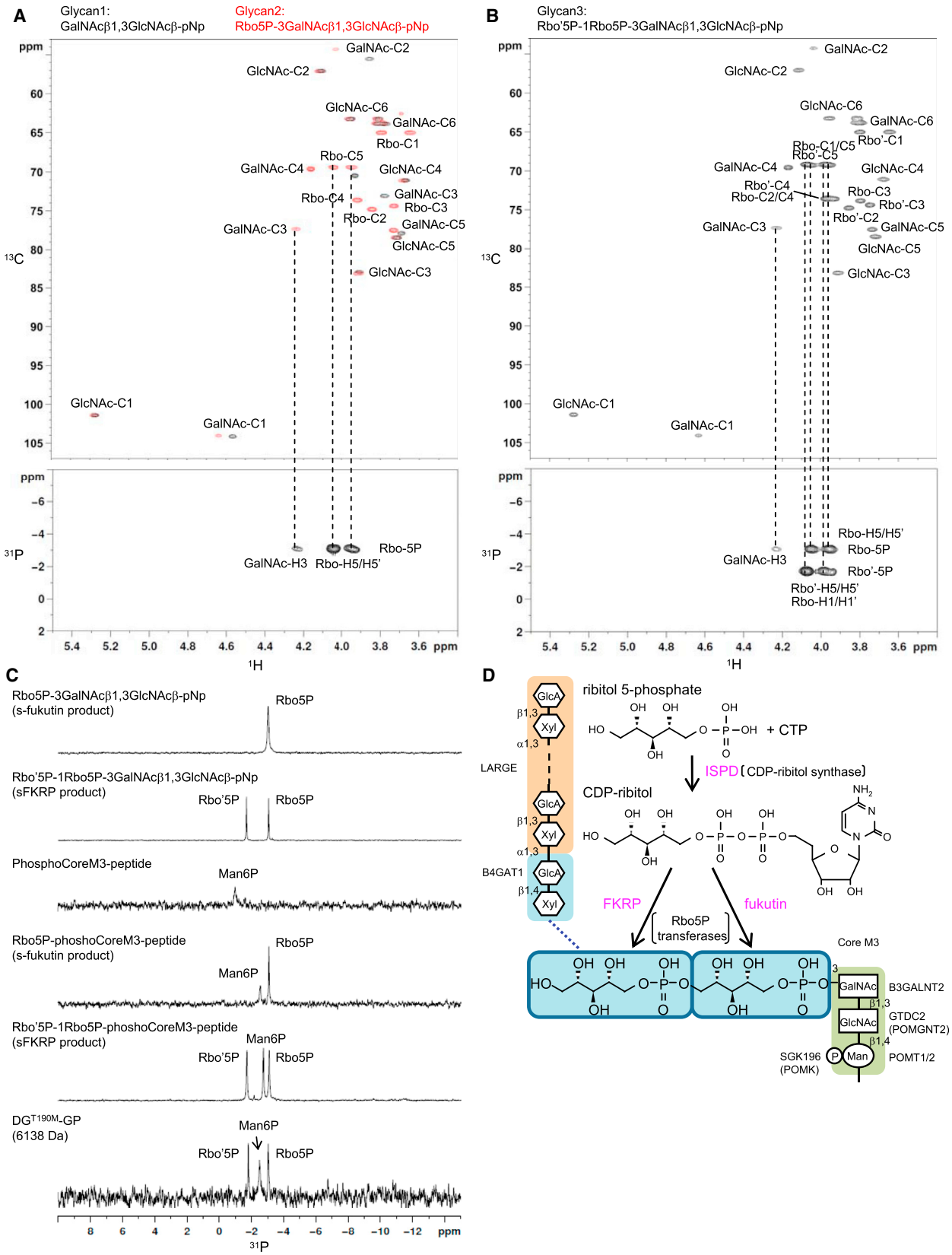

(legend on next page)

with α2-3,6,8,9-neuraminidase (Merck Millipore) at 37°C for 6 hr and then with *O*-glycosidase (New England Biolabs) at 37°C for 12 hr to remove the terminal sialic acids and *O*-GalNAc-type glycans. The samples were subjected to an anion exchange column (HiTrap Q XL beads, GE Healthcare Life Sciences) and were fractionated by stepwise elution with NH_4Ac (0.1, 0.25, 0.5, and 0.75 M). The fraction of the 0.5 M NH_4Ac elution contained the DG-GPs with Xyl/GlcA repeats, whereas the fraction of the 0.25 M NH_4Ac elution contained DG-GPs without Xyl/GlcA repeats. The fractions were freeze-dried and then analyzed by MS or further purified by HPLC. For HPLC purification, the freeze-dried samples were dissolved with 0.1% trifluoroacetic acid (TFA), loaded onto an Inertsil ODS column (2.0 × 150 mm, GL Sciences), and eluted with a linear gradient elution of acetonitrile (10%–50%) in 0.1% TFA. To obtain a short glycopeptide (QIHATPTPVK) from $DGFc^{T320K}$, the glycopeptide (QIHATPTPVKAIGPPTTAIQEPP) separated by anion exchange chromatography was digested with LEP (Wako Pure Chemicals Industries) in 50 mM ammonium bicarbonate and purified by HPLC using a PBr column (COSMOSIL, Nacalai Tesque) with a linear gradient elution of acetonitrile (10%–50%) in 0.1% TFA.

Mass Spectrometry

MALDI-TOF or nanoelectrospray ionization (nanoESI) MS was used to elucidate the glycopeptide structures. MALDI linear TOF measurements were carried out on a Voyager DE Pro MALDI-TOF mass spectrometer equipped with a nitrogen pulsed laser (337 nm) (Applied Biosystems). Typically, 0.1–1 pmol of the glycopeptide samples was dissolved in a 1 μl solution of 10 mg/ml of 2,5-dihydroxybenzoic acid (DHB) in a 0.1% TFA and 30% acetonitrile solution on a MALDI sample target and dried. The measurements were carried out in positive ion mode. For MS/MS analysis, nanoESI MS was carried out using an LTQ XL ion trap mass spectrometer (Thermo Fisher Scientific). The samples were dissolved in a 50% methanol solution and directly infused into the mass spectrometer using a PicoTip emitter (New Objective). The measurements were carried out in the negative ion mode. Typical nanoESI source conditions were 1.6 kV source voltage, −42.8 V capillary voltage, and 200°C capillary temperature.

A high-resolution MS of Structure736 was carried out on an LTQ-Orbitrap Velos Pro (Thermo Fisher Scientific) equipped with a nanoESI ion source in the negative ion mode. The spray voltage was set at 0.8 kV, with a distance of 3–5 mm between the top of the needle and the inlet of the mass spectrometer. The resolution of the equipment was set at 100,000, and the capillary temperature was set at 200°C. The samples were dissolved in a 20% methanol solution and then directly infused into the mass spectrometer using a nanoESI tip (Cellomics Tip, HUMANIX). The electron multiplier gain, Fourier transform, storage transmission, and mass accuracy were calibrated using polytyrosine (*m/z* 180.06662, *m/z* 506.19327, and *m/z* 995.38326), according to the manufacturer's instructions. The prediction of the elemental compositions from the measured accurate masses was performed by Kazusa Molecular Formula Searcher and the exact mass database of Kazusa DNA Research Institute.

Enzyme Assays for TarI and ISPD

The cDNA encoding TarI of *Bacillus subtilis* subsp. *spizizenii* TU-B-10 was chemically synthesized by GenScript, cloned into the pET-22b(+) vector (Merck Millipore), which was modified to lack the *pelB* signal sequence, and expressed in Rosetta2 *E. coli* cells (Merck Millipore). The cells were ultra-sonicated in Tris-buffered saline (TBS), and the recombinant TarI was purified using COSMOGEL His-Accept. The expression vectors for human ISPD and its mutants were transfected into HEK293T cells using Effectene. The cells were ultra-sonicated in TBS, and the ISPD proteins were purified using COSMOGEL His-Accept. The bound proteins were eluted with 0.5 M imidazole in TBS, concentrated, and buffer-exchanged into 20 mM Tris-HCl (pH 7.4) and 50 mM NaCl using an Amicon Ultra centrifugal filter unit. The ISPD reaction was performed as previously reported, with modifications (Baur et al., 2009). Briefly, the reaction mixture contained 100 mM MOPS-NaOH (pH 7.4), 10 mM $MgCl_2$, 1 mM CTP, and 2 mM Rbo5P in a total volume of 40 μl and was incubated for 2 hr at 37°C. CDP-Rbo synthase activity was monitored using an HPLC-based assay. The product was run on a 4.6 × 150 mm COSMOSIL PBr column (Nacalai Tesque) by isocratic elution with 3% methanol/97% 50 mM acetic acid-triethylamine (pH 7.3) at 30°C and detected by absorbance at 254 nm using the Prominence HPLC system. The separated peak product was collected and lyophilized for MS.

Enzyme Assay for Fukutin and FKRP

The s-fukutin or sFKRP expression vectors were transfected into HEK293T cells. The recombinant proteins were immunoprecipitated from the culture supernatants with an agarose-conjugated anti-c-Myc antibody. The proteins bound to agarose were used as the enzyme sources. The enzymatic reactions were performed in a 50 μl reaction volume containing 100 mM MES (pH 6.5), 0.5 mM CDP-Rbo, 0.1 mM acceptor peptide, 10 mM $MnCl_2$, 10 mM $MgCl_2$, 0.5% Triton X-100, and 25 μl of the enzyme-bound agarose at 37°C for 16 hr. PhosphoCoreM3-peptide and Rbo5P-phosphoCoreM3-peptide were used as acceptors for s-fukutin and sFKRP, respectively. Each product was separated by reversed-phase HPLC with a Mightysil RP-18GP Aqua column (5 × 250 mm) (Kanto Chemical). Solvent A was 0.1% TFA in distilled water, and solvent B was 0.1% TFA in acetonitrile. The peptide was eluted at a flow rate of 1 ml/min using a linear gradient of 0%–40% solvent B. The peptide separation was monitored by absorbance at 214 nm, and the products P1 and P2 were analyzed by MS.

For the reaction using pNp-oligosaccharides as the acceptor substrates, secreted s-fukutin and sFKRP were purified using COSMOGEL His-Accept or cOmplete His-Tag Purification Resin (Roche). The bound protein was eluted with 0.5 M imidazole in TBS, concentrated, and buffer-exchanged into 20 mM Tris-HCl (pH 7.4) and 50 mM NaCl using an Amicon Ultra centrifugal filter unit. The s-fukutin enzymatic reaction was performed in 2 mM GalNAcβ1,3GlcNAcβ-pNp (Tokyo Chemical Industry), 4 mM CDP-Rbo, 10 mM $MnCl_2$, 10 mM $MgCl_2$, and 100 mM MOPS-NaOH (pH 7.4) for 16 hr at 37°C. The product was run on a 4.6 × 150 mm COSMOSIL $5C_{18}$-AR-II column (Nacalai Tesque) by isocratic elution with 12.5% acetonitrile/87.5% 50 mM ammonium acetate (pH 4.0) at 30°C and detected by measuring the absorbance at 300 nm using an HPLC system. The product was collected and lyophilized for MS and NMR analyses. The FKRP enzymatic reaction was performed in 1 mM Rbo5P-3GalNAcβ1,3GlcNAcβ-pNp (s-fukutin product), 2 mM CDP-Rbo, 10 mM $MnCl_2$, 10 mM $MgCl_2$, and 100 mM MOPS-NaOH (pH 7.4) for 16 hr at 37°C. The product was run on a 4.6 × 150 mm COSMOSIL $5C_{18}$-AR-II column by linear gradient elution with 0%–30% acetonitrile/100%–70% 20 mM triethylamine acetate (pH 7.0) for 30 min at 30°C and detected by measuring the absorbance at 300 nm using HPLC system. The separated peak sample was collected and lyophilized for MS and NMR analyses.

NMR Analysis

The NMR spectra of pNP-derivatives and glycopeptides were recorded with 500 and 600 MHz spectrometers (BrukerBioSpin) using a 5-mm TXI cryogenic

Figure 6. Structure of the Tandem Rbo5P Moiety

(A and B) 2D ^{1}H-^{13}C HSQC and ^{1}H-^{31}P HMBC spectra for the s-fukutin (A) and sFKRP (B) products. NMR signals of the s-fukutin acceptor substrate (Glycan1: GalNAcβ1,3GlcNAcβ-pNp, black signals) and s-fukutin reaction product (Glycan2: Rbo5P-3GalNAcβ1,3GlcNAcβ-pNp, red signals) are shown in layers (A). NMR spectra of the sFKRP product (Glycan3: Rbo'5P-1Rbo5P-3GalNAcβ1,3GlcNAcβ-pNp) are shown (B).

(C) 1D ^{31}P-NMR analysis. The s-fukutin and sFKRP products from the acceptor substrates (GalNAcβ1,3GlcNAcβ-pNp and phosphoCoreM3-peptide) and purified DG^{T190M}-GP6138 were analyzed. The variations in the ^{31}P chemical shift of the Man6P group between samples are most likely due to the differences in the pH of each sample, which could influence the chemical shift (Mo et al., 2011).

(D) Schematic representation of the enzymatic activities of ISPD, fukutin, and FKRP, and the structure of the tandem Rbo5P moiety.

See also Figure S5.

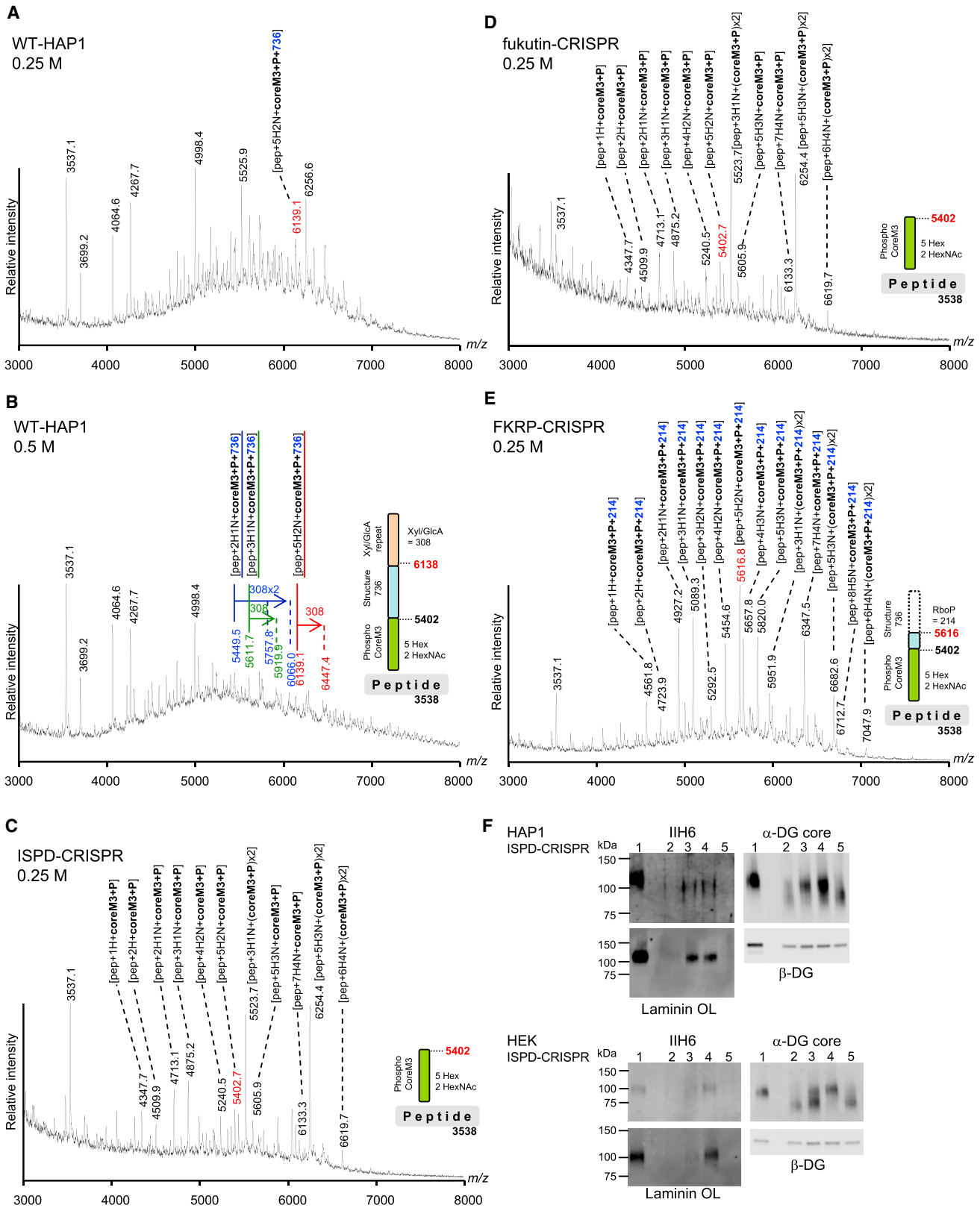

(legend on next page)

probe, a BBO probe, and a Prodigy probe. The probe temperature was set at 25°C. The samples were dissolved in D_2O (99.99 atom% D), and the ^{1}H chemical shifts were reported relative to the external standard of 4,4-dimethyl-4-silapentane-1-sulfonic acid. The ^{13}C and ^{31}P chemical shifts were calibrated using an indirect reference based on the X/^{1}H resonance ratio of 0.251449530 ($^{13}C/^{1}H$) and 0.404808636 ($^{31}P/^{1}H$). NMR signals were assigned by a series of one- and two-dimensional measurements including 1D ^{1}H, 1D ^{31}P, 2D ^{1}H-^{1}H double quantum filtered-correlation spectroscopy (DQF-COSY), homonuclear Hartmann-Hahn spectroscopy (HOHAHA), nuclear Overhauser effect spectroscopy (NOESY), ^{1}H-^{13}C HSQC, ^{1}H-^{13}C HSQC-total correlation spectroscopy (TOCSY), and ^{1}H-^{31}P HMBC spectra. The NMR data were processed with XWIN-NMR (ver. 3.5) and TopSpin (ver 2.1), and the spectra were displayed using XWIN-PLOT (ver. 3.5).

Animal Study

All animal procedures were approved by the Animal Care and Use Committee of Kobe University Graduate School of Medicine in accordance with the guidelines of the Ministry of Education, Culture, Sports, Science and Technology (MEXT) and the Japan Society for the Promotion of Science (JSPS).

SUPPLEMENTAL INFORMATION

Supplemental Information includes Supplemental Experimental Procedures and six figures and can be found with this article online at http://dx.doi.org/10.1016/j.celrep.2016.02.017.

AUTHOR CONTRIBUTIONS

M.K., K.K., M.T., H.M., and A.K. designed the project, carried out the experimental work, analyzed and interpreted the data, and wrote the manuscript. Particularly, M.K. and A.K. generated the essential reagents for structural analysis; K.K. and H.M. identified the enzyme activities and generated the glycopeptides for NMR; and M.T. performed the MS experiments. Y.Y. performed the NMR experiments and wrote the manuscript. J.F. and Y.S. conducted the MS experiments and analyzed the data. K.A.-M. performed the enzyme assay. M.M. and H.K. generated the essential reagents. Y.W., T.E., and T.T. designed the project, edited the manuscript, and jointly supervised the research. Y.W. is responsible for the MS studies. T.E. is responsible for the enzyme studies. T.T. is responsible for all the reagents and data. All authors discussed the data and the manuscript.

ACKNOWLEDGMENTS

We thank Drs. Nana Kawasaki and Noritaka Hashii for the MS studies; Feibi Zeng, Kimitaka Katanazaka, Aki Miyazaki, Sachika Inoue, Mai Kondo, Chiyomi Ito, Megumi Matsuo, and Zhongpeng Lu for preparation of the DG-GPs; Yuko Ando and Hiroko Nakano for the gene editing; Tomotaka Murotani, Mai Yamada, Kie Nagayama, and Hinako Koga for the cloning and preparation of soluble enzymes; Drs. Masayuki Okuyama and Atsuo Kimura for the reagents; Dr. Hajime Sato for the ^{31}P-NMR measurement; and Dr. Helena Akiko Popiel for critical reading of the manuscript and helpful suggestions. This work was supported by the National Center of Neurology and Psychiatry (NCNP; Intramural Research Grant 26-8 to T.T. and T.E.), Japan Agency for Medical Research and Development (AMED; 15dk0310041h0002 to T.T.), Japan Society for the Promotion of Science (JSPS; 26253057 to T.T., 25293016 to T.E., 23390081 to Y.W., 15H04352 and 24687017 to M.K., 26670499 and 21689030 to K.K., 24619014 to M.T., and 24790884 to A.K.), the Ministry of Education, Culture, Sports, Science and Technology of Japan (MEXT; 26110712 to M.K. and 26110727 to H.M.), the Special Coordination Funds for Promoting Science and Technology to Y.S., and the Mizutani Foundation for Glycoscience (150171 to H.M.). A.K. contributed to this work as a former employee of Kobe University Hospital, and the opinions expressed in this work do not represent his current affiliation—Eli Lilly Japan K.K., Kobe, Japan.

Received: October 8, 2015
Revised: December 25, 2015
Accepted: January 28, 2016
Published: February 25, 2016

REFERENCES

Ackroyd, M.R., Skordis, L., Kaluarachchi, M., Godwin, J., Prior, S., Fidanboylu, M., Piercy, R.J., Muntoni, F., and Brown, S.C. (2009). Reduced expression of fukutin related protein in mice results in a model for fukutin related protein associated muscular dystrophies. Brain *132*, 439–451.

Aravind, L., and Koonin, E.V. (1999). The fukutin protein family–predicted enzymes modifying cell-surface molecules. Curr. Biol. *9*, R836–R837.

Bao, X., Kobayashi, M., Hatakeyama, S., Angata, K., Gullberg, D., Nakayama, J., Fukuda, M.N., and Fukuda, M. (2009). Tumor suppressor function of laminin-binding α-dystroglycan requires a distinct β3-N-acetylglucosaminyltransferase. Proc. Natl. Acad. Sci. USA *106*, 12109–12114.

Baur, S., Marles-Wright, J., Buckenmaier, S., Lewis, R.J., and Vollmer, W. (2009). Synthesis of CDP-activated ribitol for teichoic acid precursors in Streptococcus pneumoniae. J. Bacteriol. *191*, 1200–1210.

Brockington, M., Blake, D.J., Prandini, P., Brown, S.C., Torelli, S., Benson, M.A., Ponting, C.P., Estournet, B., Romero, N.B., Mercuri, E., et al. (2001a). Mutations in the fukutin-related protein gene (FKRP) cause a form of congenital muscular dystrophy with secondary laminin α2 deficiency and abnormal glycosylation of α-dystroglycan. Am. J. Hum. Genet. *69*, 1198–1209.

Brockington, M., Yuva, Y., Prandini, P., Brown, S.C., Torelli, S., Benson, M.A., Herrmann, R., Anderson, L.V., Bashir, R., Burgunder, J.M., et al. (2001b). Mutations in the fukutin-related protein gene (FKRP) identify limb girdle muscular dystrophy 2I as a milder allelic variant of congenital muscular dystrophy MDC1C. Hum. Mol. Genet. *10*, 2851–2859.

Brown, S., Santa Maria, J.P., Jr., and Walker, S. (2013). Wall teichoic acids of gram-positive bacteria. Annu. Rev. Microbiol. *67*, 313–336.

Cao, W., Henry, M.D., Borrow, P., Yamada, H., Elder, J.H., Ravkov, E.V., Nichol, S.T., Compans, R.W., Campbell, K.P., and Oldstone, M.B. (1998).

Figure 7. Abnormal RboP Glycosylation in Cells with Defects in the α-Dystroglycanopathy Genes and a Possible Therapeutic Strategy Involving CDP-Rbo Supplementation

(A–E) MS of DG^{WT}-GPs expressed in normal HAP1 (A and B) and HAP1 cells with defects in *ISPD* (C), *fukutin* (D), and *FKRP* (E). (A, C–E) GPs in the 0.25 M NH_4Ac eluates. (B) GPs in the 0.5 M NH_4Ac eluate. The ions containing Structure736 are indicated in red, blue, and green (A and B). The data also suggested that the Xyl/GlcA units were modified on these GPs (arrows in B). The ions containing phosphoCoreM3 are indicated with their estimated compositions in parentheses (C–E). Ions indicated in red correspond to GP6138 (see Figures 1 and 2A), GP6138 with a Xyl/GlcA unit, or GP6138 without Structure736. pep, peptide; H, Hex; N, HexNAc; P, phosphate. Note that variations exist in the Hex/HexNAc modification patterns on DG-GPs (indicated in parentheses).

(F) Rescue of the functional glycosylation of α-DG in *ISPD*-deficient cells by CDP-Rbo supplementation. *ISPD*-deficient HAP1 or HEK293 cells were treated with exogenous CDP-Rbo. The α-DG preparations were analyzed by western blotting with antibodies to DGs and by the laminin overlay (OL) assay. Lane 1, normal control; lane 2, *ISPD*-deficient; lane 3, *ISPD*-deficient cells with CDP-Rbo; lane 4, *ISPD*-deficient cells with CDP-Rbo and Lipofectamine 2000; lane 5, *ISPD*-deficient cells with Lipofectamine 2000.

See also Figure S6.

Identification of α-dystroglycan as a receptor for lymphocytic choriomeningitis virus and Lassa fever virus. Science *282*, 2079–2081.

Chiba, A., Matsumura, K., Yamada, H., Inazu, T., Shimizu, T., Kusunoki, S., Kanazawa, I., Kobata, A., and Endo, T. (1997). Structures of sialylated O-linked oligosaccharides of bovine peripheral nerve α-dystroglycan. The role of a novel O-mannosyl-type oligosaccharide in the binding of α-dystroglycan with laminin. J. Biol. Chem. *272*, 2156–2162.

Cirak, S., Foley, A.R., Herrmann, R., Willer, T., Yau, S., Stevens, E., Torelli, S., Brodd, L., Kamynina, A., Vondracek, P., et al.; UK10K Consortium (2013). ISPD gene mutations are a common cause of congenital and limb-girdle muscular dystrophies. Brain *136*, 269–281.

Cohn, R.D., Henry, M.D., Michele, D.E., Barresi, R., Saito, F., Moore, S.A., Flanagan, J.D., Skwarchuk, M.W., Robbins, M.E., Mendell, J.R., et al. (2002). Disruption of DAG1 in differentiated skeletal muscle reveals a role for dystroglycan in muscle regeneration. Cell *110*, 639–648.

Esapa, C.T., Benson, M.A., Schröder, J.E., Martin-Rendon, E., Brockington, M., Brown, S.C., Muntoni, F., Kröger, S., and Blake, D.J. (2002). Functional requirements for fukutin-related protein in the Golgi apparatus. Hum. Mol. Genet. *11*, 3319–3331.

Goddeeris, M.M., Wu, B., Venzke, D., Yoshida-Moriguchi, T., Saito, F., Matsumura, K., Moore, S.A., and Campbell, K.P. (2013). LARGE glycans on dystroglycan function as a tunable matrix scaffold to prevent dystrophy. Nature *503*, 136–140.

Hara, Y., Balci-Hayta, B., Yoshida-Moriguchi, T., Kanagawa, M., Beltrán-Valero de Bernabé, D., Gündeşli, H., Willer, T., Satz, J.S., Crawford, R.W., Burden, S.J., et al. (2011a). A dystroglycan mutation associated with limb-girdle muscular dystrophy. N. Engl. J. Med. *364*, 939–946.

Hara, Y., Kanagawa, M., Kunz, S., Yoshida-Moriguchi, T., Satz, J.S., Kobayashi, Y.M., Zhu, Z., Burden, S.J., Oldstone, M.B.A., and Campbell, K.P. (2011b). Like-acetylglucosaminyltransferase (LARGE)-dependent modification of dystroglycan at Thr-317/319 is required for laminin binding and arenavirus infection. Proc. Natl. Acad. Sci. USA *108*, 17426–17431.

Ibraghimov-Beskrovnaya, O., Ervasti, J.M., Leveille, C.J., Slaughter, C.A., Sernett, S.W., and Campbell, K.P. (1992). Primary structure of dystrophin-associated glycoproteins linking dystrophin to the extracellular matrix. Nature *355*, 696–702.

Inamori, K., Yoshida-Moriguchi, T., Hara, Y., Anderson, M.E., Yu, L., and Campbell, K.P. (2012). Dystroglycan function requires xylosyl- and glucuronyltransferase activities of LARGE. Science *335*, 93–96.

Jae, L.T., Raaben, M., Riemersma, M., van Beusekom, E., Blomen, V.A., Velds, A., Kerkhoven, R.M., Carette, J.E., Topaloglu, H., Meinecke, P., et al. (2013). Deciphering the glycosylome of dystroglycanopathies using haploid screens for lassa virus entry. Science *340*, 479–483.

Kanagawa, M., Saito, F., Kunz, S., Yoshida-Moriguchi, T., Barresi, R., Kobayashi, Y.M., Muschler, J., Dumanski, J.P., Michele, D.E., Oldstone, M.B.A., and Campbell, K.P. (2004). Molecular recognition by LARGE is essential for expression of functional dystroglycan. Cell *117*, 953–964.

Kanagawa, M., Yu, C.C., Ito, C., Fukada, S., Hozoji-Inada, M., Chiyo, T., Kuga, A., Matsuo, M., Sato, K., Yamaguchi, M., et al. (2013). Impaired viability of muscle precursor cells in muscular dystrophy with glycosylation defects and amelioration of its severe phenotype by limited gene expression. Hum. Mol. Genet. *22*, 3003–3015.

Kobayashi, K., Nakahori, Y., Miyake, M., Matsumura, K., Kondo-Iida, E., Nomura, Y., Segawa, M., Yoshioka, M., Saito, K., Osawa, M., et al. (1998). An ancient retrotransposal insertion causes Fukuyama-type congenital muscular dystrophy. Nature *394*, 388–392.

Kuchta, K., Knizewski, L., Wyrwicz, L.S., Rychlewski, L., and Ginalski, K. (2009). Comprehensive classification of nucleotidyltransferase fold proteins: identification of novel families and their representatives in human. Nucleic Acids Res. *37*, 7701–7714.

Kuga, A., Kanagawa, M., Sudo, A., Chan, Y.M., Tajiri, M., Manya, H., Kikkawa, Y., Nomizu, M., Kobayashi, K., Endo, T., et al. (2012). Absence of post-phosphoryl modification in dystroglycanopathy mouse models and wild-type tissues expressing non-laminin binding form of α-dystroglycan. J. Biol. Chem. *287*, 9560–9567.

Kurahashi, H., Taniguchi, M., Meno, C., Taniguchi, Y., Takeda, S., Horie, M., Otani, H., and Toda, T. (2005). Basement membrane fragility underlies embryonic lethality in fukutin-null mice. Neurobiol. Dis. *19*, 208–217.

Manya, H., Chiba, A., Yoshida, A., Wang, X., Chiba, Y., Jigami, Y., Margolis, R.U., and Endo, T. (2004). Demonstration of mammalian protein O-mannosyltransferase activity: coexpression of POMT1 and POMT2 required for enzymatic activity. Proc. Natl. Acad. Sci. USA *101*, 500–505.

Matsumoto, H., Hayashi, Y.K., Kim, D.S., Ogawa, M., Murakami, T., Noguchi, S., Nonaka, I., Nakazawa, T., Matsuo, T., Futagami, S., et al. (2005). Congenital muscular dystrophy with glycosylation defects of alpha-dystroglycan in Japan. Neuromuscul. Disord. *15*, 342–348.

Michele, D.E., Barresi, R., Kanagawa, M., Saito, F., Cohn, R.D., Satz, J.S., Dollar, J., Nishino, I., Kelley, R.I., Somer, H., et al. (2002). Post-translational disruption of dystroglycan-ligand interactions in congenital muscular dystrophies. Nature *418*, 417–422.

Miller, M.R., Ma, D., Schappet, J., Breheny, P., Mott, S.L., Bannick, N., Askeland, E., Brown, J., and Henry, M.D. (2015). Downregulation of dystroglycan glycosyltransferases LARGE2 and ISPD associate with increased mortality in clear cell renal cell carcinoma. Mol. Cancer *14*, 141.

Mo, K.F., Fang, T., Stalnaker, S.H., Kirby, P.S., Liu, M., Wells, L., Pierce, M., Live, D.H., and Boons, G.J. (2011). Synthetic, structural, and biosynthetic studies of an unusual phospho-glycopeptide derived from α-dystroglycan. J. Am. Chem. Soc. *133*, 14418–14430.

Moore, S.A., Saito, F., Chen, J., Michele, D.E., Henry, M.D., Messing, A., Cohn, R.D., Ross-Barta, S.E., Westra, S., Williamson, R.A., et al. (2002). Deletion of brain dystroglycan recapitulates aspects of congenital muscular dystrophy. Nature *418*, 422–425.

Negm, F.B., and Marlow, G.C. (1985). Partial purification and characterization of d-ribose-5-phosphate reductase from Adonis vernalis L. Leaves. Plant Physiol. *78*, 758–761.

Praissman, J.L., Live, D.H., Wang, S., Ramiah, A., Chinoy, Z.S., Boons, G.J., Moremen, K.W., and Wells, L. (2014). B4GAT1 is the priming enzyme for the LARGE-dependent functional glycosylation of α-dystroglycan. eLife *3*, e03943.

Quijano-Roy, S., Martí-Carrera, I., Makri, S., Mayer, M., Maugenre, S., Richard, P., Berard, C., Viollet, L., Leheup, B., Guicheney, P., et al. (2006). Brain MRI abnormalities in muscular dystrophy due to FKRP mutations. Brain Dev. *28*, 232–242.

Roscioli, T., Kamsteeg, E.J., Buysse, K., Maystadt, I., van Reeuwijk, J., van den Elzen, C., van Beusekom, E., Riemersma, M., Pfundt, R., Vissers, L.E.L.M., et al. (2012). Mutations in ISPD cause Walker-Warburg syndrome and defective glycosylation of α-dystroglycan. Nat. Genet. *44*, 581–585.

Singh, J., Itahana, Y., Knight-Krajewski, S., Kanagawa, M., Campbell, K.P., Bissell, M.J., and Muschler, J. (2004). Proteolytic enzymes and altered glycosylation modulate dystroglycan function in carcinoma cells. Cancer Res. *64*, 6152–6159.

Tachikawa, M., Kanagawa, M., Yu, C.C., Kobayashi, K., and Toda, T. (2012). Mislocalization of fukutin protein by disease-causing missense mutations can be rescued with treatments directed at folding amelioration. J. Biol. Chem. *287*, 8398–8406.

Taniguchi-Ikeda, M., Kobayashi, K., Kanagawa, M., Yu, C.C., Mori, K., Oda, T., Kuga, A., Kurahashi, H., Akman, H.O., DiMauro, S., et al. (2011). Pathogenic exon-trapping by SVA retrotransposon and rescue in Fukuyama muscular dystrophy. Nature *478*, 127–131.

Wiggins, C.A., and Munro, S. (1998). Activity of the yeast MNN1 alpha-1,3-mannosyltransferase requires a motif conserved in many other families of glycosyltransferases. Proc. Natl. Acad. Sci. USA *95*, 7945–7950.

Willer, T., Lee, H., Lommel, M., Yoshida-Moriguchi, T., de Bernabe, D.B., Venzke, D., Cirak, S., Schachter, H., Vajsar, J., Voit, T., et al. (2012). ISPD

loss-of-function mutations disrupt dystroglycan O-mannosylation and cause Walker-Warburg syndrome. Nat. Genet. *44*, 575–580.

Willer, T., Inamori, K., Venzke, D., Harvey, C., Morgensen, G., Hara, Y., Beltrán Valero de Bernabé, D., Yu, L., Wright, K.M., and Campbell, K.P. (2014). The glucuronyltransferase B4GAT1 is required for initiation of LARGE-mediated α-dystroglycan functional glycosylation. eLife *3*, e03941.

Yoshida, A., Kobayashi, K., Manya, H., Taniguchi, K., Kano, H., Mizuno, M., Inazu, T., Mitsuhashi, H., Takahashi, S., Takeuchi, M., et al. (2001). Muscular dystrophy and neuronal migration disorder caused by mutations in a glycosyltransferase, POMGnT1. Dev. Cell *1*, 717–724.

Yoshida-Moriguchi, T., and Campbell, K.P. (2015). Matriglycan: a novel polysaccharide that links dystroglycan to the basement membrane. Glycobiology *25*, 702–713.

Yoshida-Moriguchi, T., Yu, L., Stalnaker, S.H., Davis, S., Kunz, S., Madson, M., Oldstone, M.B.A., Schachter, H., Wells, L., and Campbell, K.P. (2010). O-mannosyl phosphorylation of α-dystroglycan is required for laminin binding. Science *327*, 88–92.

Yoshida-Moriguchi, T., Willer, T., Anderson, M.E., Venzke, D., Whyte, T., Muntoni, F., Lee, H., Nelson, S.F., Yu, L., and Campbell, K.P. (2013). SGK196 is a glycosylation-specific O-mannose kinase required for dystroglycan function. Science *341*, 896–899.